# Storm Surges Beach Vulnerability Index Along the Coastline of Rio de Janeiro City, From Leme to Macumba Beaches: Contributions to Coastal Management

# *Índice de Vulnerabilidade das Praias a Ressacas ao Longo da Orla da Cidade do Rio de Janeiro, das praias do Leme à Macumba: Contribuições para a Gestão Costeira*

**Pedro Antonio da Silva Piacesi**[ac], **Flavia Moraes Lins-de-Barros**[ad], **Pedro Torres Costa**[be]

[a]Graduate Program in Geography - Federal University of Rio de Janeiro (UFRJ), [b]Department of Geography - Federal University of Rio de Janeiro (UFRJ)
[c]pedroaspiacesi@gmail.com, [d]flaviamlb@gmail.com, [e]pedrot85@gmail.com



**Abstract**

Storm surge is a phenomenon of particular concern for the population, media, authorities, and coastal management. Sandy beaches, depositional environments located at the land-sea interface, are directly exposed to the action of storm waves. In Rio de Janeiro, this issue is exacerbated as its beaches are directly exposed to high-energy waves from the south, typical of storm surges. Using a multicriteria approach, this study presents a methodology for assessing beach vulnerability to storm surges through the development and application of an index based on two components: beach exposure and adaptive capacity. The index was applied to the urbanized oceanic beaches of Rio de Janeiro. The exposure subindex evaluates wave incidence, wave collision potential, and coastal slope. The adaptive capacity subindex includes variables such as grain size, coastal elevation and beach width. Results indicate that 27.5% of the study area has very high exposure to storm waves, 69.4% shows high adaptive capacity, and 7.9% demonstrates high vulnerability, particularly at Macumba, Leblon, and Arpoador beaches. The importance of vulnerability studies for coastal management is emphasized, contributing to the development of early warning systems and urban planning. Nature-based solutions, such as dune restoration, are recommended to enhance beach system resistance. This approach supports sustainable coastal management, reducing reliance on engineering solutions and promoting long-term resistance to storm impacts.

**Keywords**: Storm surge; Beach vulnerability; Coastal management.

**Resumo**

Ressaca do mar é um fenômeno de especial atenção para a população, mídia, autoridades e, logo, à gestão costeira. As praias arenosas, ambientes de deposição de material sedimentar localizadas na interface terra-mar, são diretamente expostas à ação de ondas de ressaca. No Rio de Janeiro, esse caso se agrava uma vez que suas praias estão diretamente expostas a ondas de alta energia provenientes de sul, típicas de ressaca. Utilizando uma abordagem multicritério, o presente trabalho apresenta uma metodologia para avaliação da vulnerabilidade de praias às ressacas a partir da construção e aplicação de um índice baseado em duas componentes: exposição e capacidade adaptativa das praias. O índice foi aplicado às praias oceânicas urbanizadas da cidade do Rio de Janeiro. O subíndice de exposição avalia a incidência de ondas, o potencial de colisão de ondas e a inclinação da costa. O subíndice de capacidade adaptativa inclui variáveis como tamanho de grão, elevação da costa e largura da praia. Resultados indicam que 27,5% da área de estudo possui exposição muito alta às ondas de ressaca, 69,4% possui alta capacidade adaptativa e 7,9% possui alta vulnerabilidade, particularmente nas praias da Macumba, Leblon e Arpoador. Enfatiza-se a importância de estudos de vulnerabilidade para a gestão costeira, contribuindo para o desenvolvimento de sistemas de alerta preliminares e para o planejamento urbano. Soluções baseadas na natureza, como restauração de dunas, são recomendadas para aumentar a resistência do sistema praial. Esta abordagem apoia a gestão costeira sustentável, reduzindo a dependência de soluções de engenharia e promovendo resistência a longo prazo a impactos de tempestades.

**Palavras-chave:** Ressacas do mar; Vulnerabilidade de praias; Gestão costeira.

https://doi.org/10.5380/qeg.v16i1.97981

## 1. Introduction

Sandy beaches are dynamic depositional environments composed of loose, permeable sediments that are continuously shaped by marine, terrestrial, atmospheric and astronomical processes. These processes influence the volume and morphology of beaches to different degrees. Typically composed of quartz sand, these unconsolidated sediments serve as key zones for wave energy dissipation (Bird 2008). Significant changes in beach morphology are often driven by high-energy events, such as storm waves and storm surges, which are characterized by elevated sea levels due to astronomical and meteo-oceanographic factors. Combined with wave action, these events can cause substantial impacts on coastal systems, resulting in both natural and socio-economic losses (Lima et al. 2021). As a result, the coastal zone — and sandy beaches, in particular — are widely recognized as inherently unstable and highly vulnerable environments (Alexandrakis & Poulos 2014, Lins-de-Barros et al. 2020, Lins-de-Barros 2017).

The study of such environments requires a dual perspective. On the one hand, sandy beaches are exposed to oceanographic and meteorological phenomena, such as storm surges, which can induce coastal erosion and flooding. On the other hand, their geomorphological characteristics provide varying degrees of resistance and adaptation to extreme events and rising sea levels. The resulting beach morphology reflects the ongoing interaction of these diverse processes, which vary over time.

In Rio de Janeiro, storm surge events have been documented since the early $20^{th}$ century. With the intense urbanization of the city’s coastline, these events have become an increasing concern for residents, policymakers, and researchers. According to Muehe et al. (2018), qualitative observations of erosional and recovery patterns reveal that much of Rio de Janeiro’s coastal stretch is prone to erosion. Understanding the spatial distribution and frequency of storm surges, along with the vulnerability of beaches to these events, is critical for formulating coastal management strategies. Such knowledge supports the development of public policies aimed at ensuring the safety of beachgoers and protecting infrastructure near the shoreline, making it an essential component of territorial planning (Lima 2022).

As Hinkel & Klein (2009 p. 384) states “Knowledge on coastal vulnerability enables scientists and policymakers to anticipate impacts that could emerge as a result of sea-level rise and other effects of climate change. It can thus help to prioritize management efforts that need to be undertaken to minimize risks or to mitigate possible consequences.”. So, it can support the anticipation of climate-related impacts and the definition of management priorities.

However, as recent events in Brazil have demonstrated, merely identifying risks is not enough to prevent damage. A more holistic approach is needed, one that integrates technical assessments with effective governance and the implementation of public policies. Several coastal disasters in the past decade have occurred despite prior vulnerability assessments, revealing critical gaps between knowledge production and decision-making.

A recent notable example is the tragedy in São Sebastião (SP), where, prior to the February 2023 landslides, researchers and institutions had already issued warnings about the geotechnical risks associated with unregulated hillside occupation (Marandola Jr. et al. 2013) and some areas in the region were considered highly vulnerable (Anazawa et al. 2011). The risks were widely recognized, and in 2020 the Public Prosecutor’s Office of the State of São Paulo alerted the municipal government of São Sebastião to the irregular occupation of the Vila Sahy hillside (Xavier 2023). In 2021, when demanding corrective measures, the agency classified the situation as “a disaster foretold” (Xavier 2023, G1 Vale do Paraíba e Região 2023). Still, no significant or sufficient preventive actions were taken, resulting in dozens of deaths and the forced displacement of residents.

Another recent case is the massive flooding that struck the state of Rio Grande do Sul in 2024, affecting 478 of the state's 497 municipalities, impacting 2.4 million people, and resulting in over 180 deaths (Caleffi et al. 2024, G1 RS 2025). Like the events in the Serra do Mar in 2023, the disaster had been anticipated by specialists (Uchoa 2024). Previous studies had already pointed to the region’s susceptibility to flooding (Marth et al. 2016, Moura et al. 2016). Marengo et al. (2024) highlight the recurrence of flooding in the state, and the “Brazil 2040” report, published in 2015, had already warned of an increased risk of floods in Brazil’s southern region (Dias 2024). Despite the existence of the Flood Protection System, created in the 1970s (Marengo et al. 2024), it failed to withstand the water volume, mainly due to lack of maintenance and design flaws (Rodrigues 2024). After the disaster, the government launched the “Plano Rio Grande” to support recovery efforts. However, progress has been slow, and according to an analysis by the climate change startup Kaz Tech, none of the projects under the plan focus on disaster prevention (Oliveira 2025), reinforcing criticism that the response has been predominantly reactive.

In this context, this study aims to evaluate the coastal vulnerability of Rio de Janeiro’s oceanic beaches, from Leme to Macumba, to storm surge impacts through the development of a physical vulnerability index for beaches. The findings are expected to support the implementation of a Storm Impact Alert System (SAIR, in Portuguese) for the city, as well to produce technical knowledge, support decision-making processes related to coastal erosion management and promote its effective integration into public policies focused on prevention and adaptation.

## 2. Study area

The study area comprises 48.5 km of the oceanic coastline of Rio de Janeiro, Brazil (Fig. 1). It is limited to the east by Ponta do Leme and to the west by the Morto River channel at Macumba Beach. From east to west, the study area includes the beach arcs of Copacabana-Leme (CLA), Leblon-Ipanema-Arpoador (LIA), São Conrado (SCB), Recreio-Reserva-Barra da Tijuca (RBT) and Macumba (MCB).

The study area is part of the Coastal Barriers Macrocompartment, which extends from Cabo Frio to Marambaia, following a predominantly east-west orientation (Muehe et al. 2018). A key feature of this region is the presence of double transgressive coastal barriers, accompanied by coastal lagoons situated inland. The most important examples include Rodrigo de Freitas Lagoon, located behind the Leblon-Ipanema-Arpoador beach arc, and Marapendi Lagoon, positioned behind the Recreio-Reserva-Barra da Tijuca segment. Further inland, the Jacarepaguá and Tijuca lagoons are situated behind Marapendi Lagoon, collectively forming what is recognized as a double coastal barriers system (Muehe & Valentini 1998, Dias & Kjerfve 2009). These features date back to the last marine transgression, approximately 7,000 years ago, when sea levels were higher than present (Muehe & Valentini 1998, Martin & Bittencourt 1982, Lins-de-Barros & Parente-Ribeiro 2018).

The area displays various morphodynamic stages (as defined by Wright & Short (1984)) along its beach arcs. On Copacabana and Leblon beaches, Bulhões (2006) identified reflective and low tide terrace morphodynamic stages. The beaches of Ipanema and Recreio dos Bandeirantes exhibit stages that vary between reflective, low tide terrace, transverse-bar and beach, and longshore bar-trough stages. São Conrado Beach alternates primarily between longshore bar-trough, low tide terrace, and transverse-bar and beach stages. In the Recreio-Reserva-Barra da Tijuca beach arc, the most predominant morphodynamic stages include low tide terrace, transverse-bar and beach, and reflective stages. Carvalho (2019) noted that Macumba Beach is largely dominated by rhythmic bar and beach stage, followed by longshore bar-trough, reflective, and transverse-bar and beach stages.

Grain size distribution in the study area also varies significantly. According to Pena (2017), coarse sand predominates on Macumba Beach. In the Recreio-Reserva-Barra da Tijuca arc, grain-size range from very fine to very coarse sand, with the predominance of medium and coarse sand (Carvalho 2019). Medium-sized sand dominate São Conrado Beach, while the Leblon-Ipanema-Arpoador arc exhibits a variation from coarse to fine sand. Primary data from the Marine Geography Laboratory of UFRJ indicate that medium sand is predominant along the Copacabana-Leme arc.

### 2.1 Meteo-oceanographic characteristics

The study area, like the entire southeastern region of Brazil and its adjacent oceanic waters, is strongly influenced year-round by the South Atlantic Subtropical Anticyclone (SASA) (Muehe et al. 2018). This influence is compounded by frontal systems and extratropical cyclones originating from the southeast (SE) and southwest (SW), which generate high-energy wave conditions typical of storm surge conditions (Muehe et al. 1998 p. 484).

Due to the predominantly linear orientation of the Coastal Barriers Macrocompartment, the coastline — and, consequently, the oceanic beaches of Rio de Janeiro city — are particularly vulnerable to high-energy swells from the southern quadrants, which are also characteristic of storm surge events. Lima et al. (2021), in a temporal analysis covering the period from 1948 to 2008, determined that storm surges affecting the state of Rio de Janeiro are characterized by significant wave heights ranging from 2.5 m to 4.0 m, originating from SSW, with peak wave periods between 9 and 11 seconds (Fig. 2). These events are most frequent during transitional tides and are more common in the autumn months.

Analyzing wind and wave data for the Santos Basin from 1997 to 2011 using the WaveWatch III (WW3) model, Nascimento (2013) found a predominance of winds from the northeast (NE) and east (E), followed by winds from the southeast (SE). The strongest winds occurred during the summer and spring. Carvalho et al. (2021), using deep-water buoy data (CF2), identified wave directions ranging from E to WSW. Eastern waves were the most frequent, while waves from the south (S) were the most energetic, with significant wave heights exceeding 5 m and periods reaching up to 18 seconds. Storm events were primarily associated with SW-directed waves and periods exceeding 12 seconds.

Klumb-Oliveira (2024), employing the Storm Power Index (SPI) methodology proposed by Dolan & Davis (1992), identified 231 storm events in the study area between 1979 and 2013, most of which were classified as Weak or Moderate. Extreme events accounted for 3.4% of occurrences (n = 8). The return period for events between classes Weak and Severe was estimated at one year, while events classified as Severe or above had a return period of five or more years. Weak and Moderate events were observed throughout the year; Significant and Severe events were recorded between March and November, and Extreme events occurred from April to September. The average storm duration was calculated to be 27.8 hours.

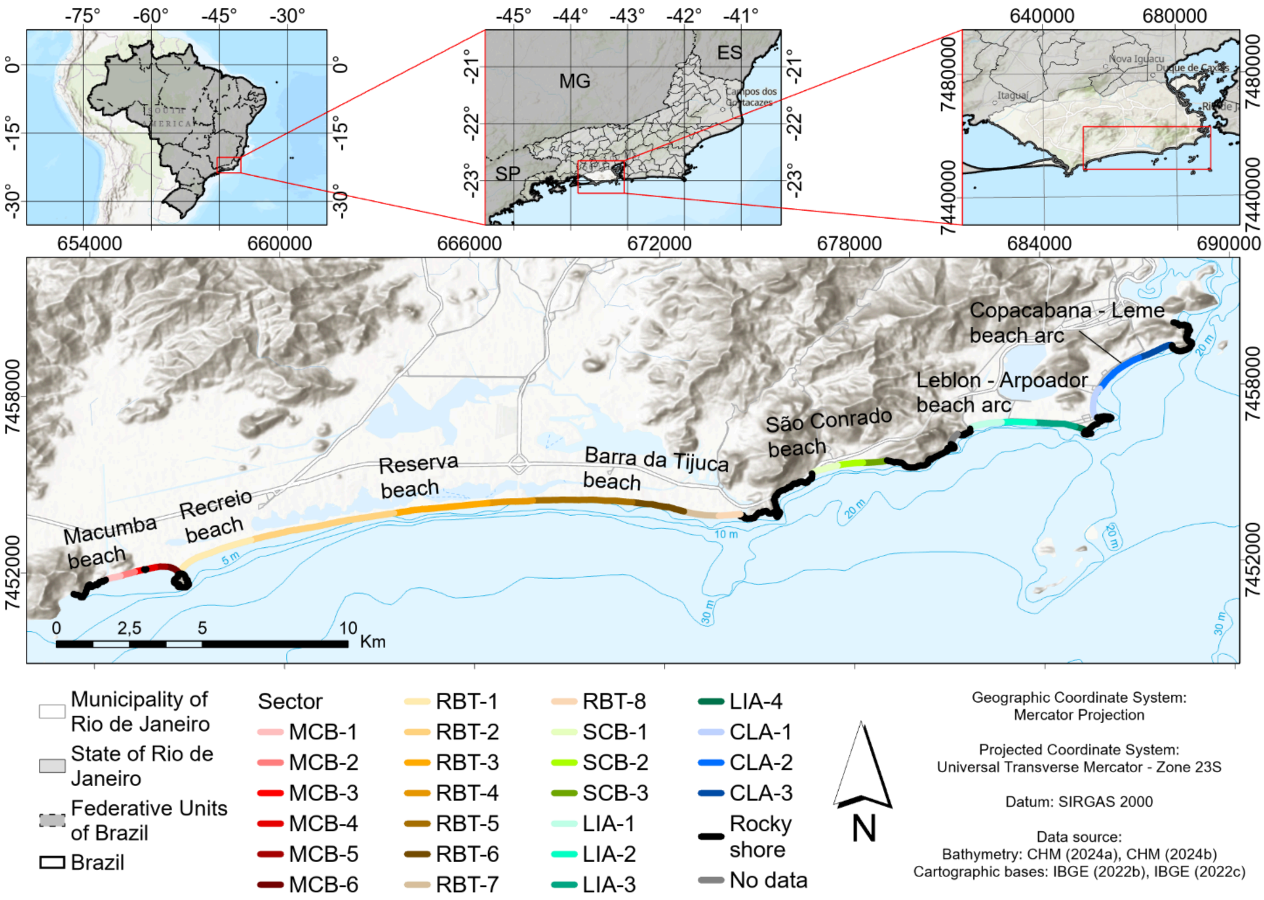


Figure 1: Study Area and Analyzed Beaches, From Leme to Macumba.

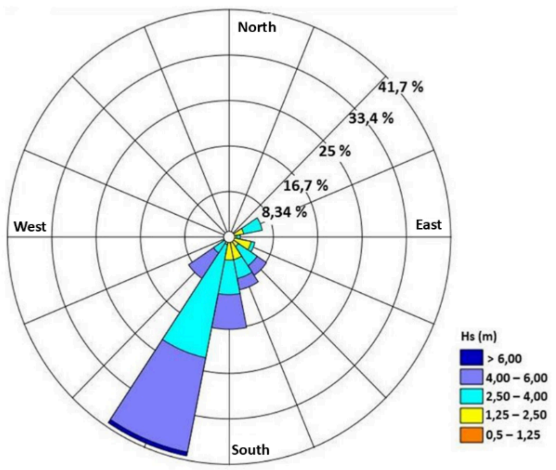


Figure 2: Directional wave rose of the highest significant wave height during storm surge events in the state of Rio de Janeiro (1948–2008). Source: Adapted from Lima et al. (2021).

Assessing data from NOAA's Climate Forecast System Reanalysis and Reforecast (CFSRR/NCEP) for the period 1979-2013, Lins-de-Barros et al. (2018) observed that at an offshore point near Saquarema (RJ), waves predominantly come from the east (45.8%) and south (44.9%), with heights between 2 and 4 m. Finally, according to the Hydrographic and Navigation Directorate (DHN), the region experiences a microtidal regime, with spring tide amplitudes reaching up to 1.5 m.

Therefore, storm surges in Rio de Janeiro result from the interaction of three key components: strong winds, ocean swell and local tides. While the region has a microtidal regime, the coincidence of southern frontal systems, low-pressure extratropical cyclones — which generate remote energetic waves —, local winds and tidal peaks (Nascimento 2013, Muehe et al. 2018) intensify wave conditions, elevate sea levels and lead to coastal impacts.

The overlap of these factors characterizes the phenomenon known as storm surge, which includes the piling up of water mass against the coast (wave setup), resulting in a temporary rise in sea level above the mean sea level. When combined with wave action, this can generate significant impacts and damages to coastal infrastructure (Lins-de-Barros et al. 2020, Lima et al. 2021). Historical data from Lima et al. (2021), Nascimento (2013), Carvalho et al. (2021), Klumb-Oliveira (2024), and Lins-de-Barros et al. (2018) confirm the seasonal pattern and energy profile of these events, highlighting the predominance of E and S waves and their recurrence in autumn and winter (Klumb-Oliveira 2024). Altogether, these factors make Rio de Janeiro's beaches especially exposed to storm surge dynamics, underlining the importance of understanding these processes for coastal management and risk mitigation.

## 3. Material and Methods

### 3.1 Coastal vulnerability terminology

The term coastal vulnerability has been widely conceptualized and debated in the literature. In general terms, vulnerability can be understood as the potential for loss, encompassing not only the degree of exposure of a system to hazards, but also its propensity to suffer harm, as well as its capacity to respond, cope, and adapt (Cutter 2011, IPCC 2023). It refers not only to the exposure of a community or environmental system to hazards, but also to its degree of susceptibility and its adaptive capacity in the face of environmental threats, in addition to the resulting impacts (Lins-de-Barros et al. 2020).

In this article, coastal vulnerability is conceptualized as the relationship between the exposure of a given coastal system to natural forcing agents and its adaptive capacity — whether physical, social, or ecological —, the latter understood as a combination of adaptation and resistance, following Adger et al. (2004), McFadden (2007) and Lins-de-Barros et al. (2020). For McFadden (2007), vulnerability can be expressed in a simple relation: vulnerability = impacts minus effect of adaptation. Thus, in line with the structure of the index proposed in this study, vulnerability is defined as the result of the interaction between the degree of exposure of the coastal system to forcing agents and its adaptive capacity to cope with such pressures, determined by the characteristics of the affected system.

### 3.2 Definition of storm surge

At present analysis, the forcing agent considered is the storm surge, defined as "a natural phenomenon induced by the accumulation of a water mass along the coast and oceanographic processes, resulting in perceptible effects on beaches or the shoreline." (Lins-de-Barros et al. 2018 p. 98).

The term storm surge used here is a translation to the concept of "ressaca do mar", a term widely used in Brazilian scientific literature. As noted by Lins-de-Barros et al. (2020), "ressaca" can carry varied and sometimes ambiguous meanings, especially in international contexts.

Lins-de-Barros et al. (2018) conducted a literature review to distinguish between ressaca do mar, maritime storms, and extreme wave events. They emphasize that not every episode involving high waves or storms qualifies as a "ressaca", since the defining criterion is the occurrence of coastal impact. Furthermore, Harley (2017) defines storm surge as "the sudden rise in water level associated with certain coastal storms, which can have catastrophic consequences for low-lying coastal areas.". Although the first defines the event by the actual occurrence of coastal damage and the second highlights the possibility of such impacts, in both cases the defining element is the association with potential coastal consequences rather than solely the meteorological or oceanographic cause. Additionally, as detailed by Lima et al. (2021), "ressacas" are associated with sea-level rise phenomena of astronomical and meteorological origin, which, combined with wave action, can cause damage or other impacts along the coastline.

Woodworth et al. (2019), as in Lima et al. (2021), adopt a more process-oriented definition, describing storm surge as a modification of sea level resulting from the combined influence of wind and atmospheric pressure, which may cause damage such as catastrophic flooding and loss of life. This definition emphasizes the physical process that may lead to such outcomes.

Paula et al. (2016 p. 1) define "ressaca" as "a natural phenomenon that can be induced by an individual or combined action of natural forcings (e.g., waves, tides, and wind)." and occurs when there is a piling up of water near the coast. The maximum water level reached — resulting from maximum wave swash and momentary sea level rise — leads to the maximum wave swash on the beach surface, contributing to fast changes in the beach profile. This definition, as in Woodworth et al. (2019), highlights the physical mechanisms involved, although it does not require the occurrence of impacts as a prerequisite for its characterization.

Therefore, the adoption of the term storm surge as a translation to "ressaca" in this article is justified as it synthesizes both the physical dynamics and the coastal consequences associated with "ressaca", in line with the conceptual definitions found in both the international (Harley 2017, Woodworth et al. 2019) and Brazilian literature (Lima et al. 2021, Lins-de-Barros et al. 2018, Lins-de-Barros et al. 2020, Paula et al. 2016).

Though, as Paula (2012) points out, meteorologically induced sea-level anomalies are commonly referred to in Brazil as "maré meteorológica", whereas the Anglo-Saxon literature uses the term storm surge in this context. Based on this distinction, the author suggests that storm surge should be considered a phenomenon associated with "ressaca", rather than a direct synonym or component of it.

### 3.3 Determination of the Beach Vulnerability Index (BVI)

The Beach Vulnerability Index (BVI) to storm surge impacts proposed in this study was developed by combining the components of "Exposure" (Ex) and "Adaptive Capacity" (AC).

Ex and AC components reflect the physical system conditions of beaches that determine the likelihood of impacts or negative effects during storm surge events. The Ex component forms a subindex composed of variables and indicators that indicate the susceptibility of a given coastal segment to wave incidence and the resulting impacts.

The AC component, on the other hand, represents the physical characteristics of beaches that provide structural resistance to the immediate effects of storm surge events. So, it is associated with the beach's ability to withstand and absorb wave energy during the event, minimizing direct and immediate damage.

The capacity of the system to return to its normal conditions — that is, the physical resilience of beaches, as defined by Fernandez et al. (2015) — was not included in the formulation of the index presented in this study. Resilience represents a post-impact characteristic — namely, the beach's ability to recover after a storm surge event. While it is a fundamental factor in assessing trends in coastal systems, resilience does not influence the immediate potential for storm surge impacts, which is the primary focus of this analysis. Therefore, although it shares the idea of "response capacity" with resilience, AC in this study does not include recovery time as a variable, as its focus is on the physical resistance present before and during the event, and not on post-impact dynamics. It is, therefore, a preventative component, related to the physical conditions of the beach at the moment the impact occurs.

The Ex and AC subindices, as well as the composite index, were developed through the mapping and grouping of indicators, defining value ranges for their variables, and applying scoring and standardization formulas based on existing literature (Gornitz 1991, Ramieri et al. 2011, Peña-Alonso et al. 2017, Dong et al. 2018, Carvalho & Guerra 2020). Beach vulnerability indexes were proposed by other authors. For example, Alexandrakis & Poulos (2014) focused their vulnerability assessment specifically on beaches, considering the predominant hydrodynamic and sedimentary processes that influence beach evolution. Andrade et al. (2019) have proposed a beach vulnerability index based on exposure wave, terrain elevation, wave power, angle of incidence and wave run up. Peña-Alonso et al. (2017) have proposed a beach geomorphological vulnerability based on the following aspects: exposure factors (human pressure and marine incidence), geomorphological susceptibility, and geomorphological resistance. The choice of variables for this research was based on these articles, adapting to local reality and data availability.

Furthermore, this study adopted an equal-weight approach for all variables. This methodological decision assumes that all variables contribute equally to coastal vulnerability, reducing subjectivity in the analysis and ensuring greater transparency and reproducibility of the methodology. This approach also follows examples from similar studies in literature, such as De Serio et al. (2018), Pantusa et al. (2018), and the classic study by Gornitz (1991). However, the application of weighting can be useful in contexts where there is robust prior knowledge about the relative influence of each variable on the vulnerability degree, a possibility that may be explored in future studies.

It is important to note that the vulnerability index presented here represents average conditions of the physical characteristics of the segments of the study area. In other words, the classification of each segment for each variable reflected its average behavior, obtained from data measured during field monitoring conducted between 2016 and 2024. Thus, the index indicates which segments are likely to be more affected by the most common storm surge events in the study area.

The segments indicated as most vulnerable are those that more frequently experience sediment stock reduction and damage. However, these effects can also be felt in segments with lower vulnerability under specific sea conditions. For example, strong waves coming from SE tend to have a greater impact on Arpoador; Leblon, however, may remain stable under these conditions and even receive sediments due to the resulting longshore transport in that direction, and vice versa (Neves et al. 2007). Moreover, combinations of more than one storm surge in a short time span can also cause more severe impacts, even on less vulnerable beaches that were in a weakened state at the time.

Additionally, anthropogenic interventions in the beach profile — such as the removal of dunes and restinga, or the construction of engineering structures on the active beach zone — can significantly change the degree of vulnerability over time, as well as the recovery time of the beach profile after erosion. Similarly, sea level rise, as shown by IPCC forecasts, can also alter the degree of vulnerability, making continuous monitoring of the study area essential.

The index, therefore, indicates vulnerability hotspots, but it is essential to develop real-time monitoring of sediment stock and transport, coupled with monitoring of oceanographic conditions, in order to generate impact alerts and support the development of an early warning system.

### 3.3.1 Index and subindices

The variables comprising the Ex and AC subindices are listed in Table 1, which also provides their data sources and the scores received by each class of the variables. For the Ex subindex, the following variables were considered: (a) beach exposure to wave incidence; (b) wave collision potential; and (c) foreshore slope.

The beach exposure to wave incidence (a) relates to the degree of exposure of beaches to storm waves and the presence or absence of natural barriers, such as islands or rocky shores. The wave collision potential (b) was defined based on the impact scale model developed by Sallenger (2000), which incorporates morphological parameters related to wave run-up. The foreshore slope (c), derived from in situ topographic profiles, determines the degree of wave energy dissipation: steeper slopes tend to reduce energy dissipation and allow for greater wave reach (run-up) on the beach profile (Sallenger op. cit.). Consequently, in this study, steeper slopes were associated with higher vulnerability levels.

The AC subindex included the following variables: (d) grain size; (e) backshore elevation; (f) backshore feature type; (g) protective beach width gradient; and (h) average beach width.

Grain size (d) is widely recognized in the literature as influencing sediment transport and erosion resistance. A higher percentage of fine sediments reduces resistance, as finer quartz sediments tend to be lighter and move more easily (Komar & Miller 1973). Thus, the presence of finer sediments contributes to reduced resistance of the beach section.

Variables (e) and (h) provide insight into a beach's resistance and recovery potential. Backshore elevation (e) acts as a natural barrier, while width (h) indicates sediment storage capacity. Sediment storage is critical because, during storms, the sand volume within the protective width is typically displaced offshore into the sandbar system. Over time, this sand gradually returns to the forebeach, facilitating natural recovery (Dong et al. 2018). This dynamic has been observed on beaches in the state of Rio de Janeiro (Muehe 2011, Filho et al. 2020).

Table 1: BVI variables, data sources, their classes, and assigned scores.

| Subindex | Variable | Class | Assigned score | Data source |
|---|---|---|---|---|
| Ex | a. Beach exposure to wave incidence | Sheltered | 1 | Satellite image |
| | | Semi-exposed | 3 | |
| | | Exposed | 5 | |
| | b. Wave collision potential | Very low | 1 | Determined from the Storm Impact Scale (Sallenger 2000) using data obtained from fieldwork |
| | | Low | 2 | |
| | | Medium | 3 | |
| | | High | 4 | |
| | | Very high | 5 | |
| | c. Foreshore slope (%) | (0, 3.5) | 1 | Data obtained from fieldwork |
| | | (3.5, 7) | 2 | |
| | | (7, 10.5) | 3 | |
| | | (10.5, 14) | 4 | |
| | | (14, ∞) | 5 | |
| AC | d. Grain size | Very coarse sand | 1 | Results from sieve analysis and secondary data (Pena 2017, Carvalho et al. 2021, Silva & Lins-de-Barros 2018) |
| | | Coarse sand | 2 | |
| | | Medium sand | 3 | |
| | | Fine sand | 4 | |
| | | Very fine sand | 5 | |
| | e. Back beach elevation (m) | (6, ∞) | 1 | Survey from topographic profiles conducted by the Marine Geography Laboratory of UFRJ and secondary data (Carvalho et al. 2021, Silva & Lins-de-Barros 2018) |
| | | (5, 6) | 2 | |
| | | (4, 5) | 3 | |
| | | (3, 4) | 4 | |
| | | (0, 3) | 5 | |
| | f. Back beach feature | Cliff | 1 | Satellite image |
| | | Vegetated foredune | 2 | |
| | | Degraded foredune | 3 | |
| | | Water Body | 4 | |
| | | Urban area | 5 | |
| | g. Protective width slope (%) | (12, ∞) | 1 | Survey from topographic profiles conducted by the Marine Geography Laboratory of UFRJ and secondary data (Carvalho et al. 2021, Silva & Lins-de-Barros 2018) |
| | | (8, 12) | 2 | |
| | | (4, 8) | 3 | |
| | | (2, 4) | 4 | |
| | | [0, 2) | 5 | |
| | h. Beach width (m) | (100, ∞) | 1 | Survey from topographic profiles conducted by the Marine Geography Laboratory of UFRJ and secondary data (Carvalho et al. 2021, Silva & Lins-de-Barros 2018) |
| | | (75, 100) | 2 | |
| | | (50, 75) | 3 | |
| | | (25, 50) | 4 | |
| | | (0, 25) | 5 | |

The protective width is defined as the horizontal distance that includes dune width, the seaward dune slope, and berm width (Dong et al. 2018). Therefore, variable (g) reflects the beach's resistance (or lack thereof) to wave collision and overwash. A steeper gradient represents a greater obstacle to wave encroachment on the beach profile.

The backshore feature type (f) assesses the characteristics of the exposed backshore and their role in wave energy dissipation. The replacement of natural barriers with artificial structures, or the degradation of dune vegetation, increases exposure and vulnerability.

Each variable was assigned a value from 1 to 5 based on its contribution to the overall vulnerability level. Each sub-index was calculated based on Equations 1 and 2.

$$Ex = (a + b + c) / VmaxEx; \quad (1)$$

$$AC = (d + e + f + g + h) / VmaxAC, \quad (2)$$

The abbreviations “a” to “h” represent the score of each variable. Vmax represents the maximum possible sum of parameter scores, achieved when each variable receives the highest score of 5. Then VmaxEx is equal to 15 (referring to the three variables of the Ex sub-index), and VmaxAC is equal to 25 (referring to the five variables of the CA sub-index).

The Ex and CA sub-indices were normalized to range between 0.2 (minimum possible value, when all variables are scored 1) and 1.0 (maximum possible value, when all variables are scored 5) (Tables 2 and 3). The range between these extremes is 0.8, which was divided into five equal classes with intervals of 0.16. These classes represent vulnerability levels: “Very low”, “Low”, “Moderate”, “High” and “Very high.”

Each class was associated with an ordinal score from 1 to 5, reflecting its contribution to the overall degree of vulnerability. For the Ex sub-index, higher values indicate a greater contribution to vulnerability, with ordinal scores ranging from 1 (Very low) to 5 (Very high). In contrast, the AC sub-index follows the opposite logic: the greater the adaptive capacity, the lower the vulnerability. Thus, its ordinal scores range from 1 (Very high) to 5 (Very low).

These ordinal scores were named ExS and ACS for the Ex and CA sub-indices, respectively. The BVI is then obtained by summing both scores (Equation 3), resulting in a total score ranging from 2 (Very low vulnerability) to 10 (Very high vulnerability). The ranges corresponding to each vulnerability level are detailed in Tables 2, 3, and 4. The final index was calculated using the following equation:

$$BVI = (ExS + CAS) \quad (3)$$

Table 2: Value ranges and corresponding classes for the Ex subindex.

| Ex score | Class | Score (ExS) |
|---|---|---|
| (0.2, 0.36) | Very low | 1 |
| (0.36, 0.52) | Low | 2 |
| (0.52, 0.68) | Moderate | 3 |
| (0.68, 0.84) | High | 4 |
| (0.84, 1) | Very high | 5 |

Table 3: Value ranges and corresponding classes for the AC subindex.

| AC score | Class | Score (ACS) |
|---|---|---|
| (0.2, 0.36) | Very high | 1 |
| (0.36, 0.52) | High | 2 |
| (0.52, 0.68) | Moderate | 3 |
| (0.68, 0.84) | Low | 4 |
| (0.84, 1) | Very low | 5 |

Table 4: Value ranges and corresponding classes for the BVI.

| Total score | Class |
|---|---|
| 2 | Extremely low |
| 3 | Very low |
| 4 | Low |
| 5 | Low - Moderate |
| 6 | Moderate |
| 7 | Moderate - High |
| 8 | High |
| 9 | Very high |
| 10 | Extremely high |

### 3.4 Smartline

The Smartline methodology was employed to map the physical characteristics of the beaches. This approach, developed by Sharples (2006) and later formalized in Sharples (2009), was initially applied to the Australian coastline. It involves the creation of simplified line-based maps that classify the coast geomorphologically while integrating variables associated with specific indicators or parameters. This method facilitates data cross-referencing and enhances the visualization of the characteristics of each coastal segment.

The Smartline subdivisions are determined whenever there is a change in the value, class, or characteristic of the indicator represented, ensuring that the level of detail in the information remains consistent across the mapped segments (Sharples 2009).

## 4. Results

### 4.1 Ex subindex

a) Beach exposure to wave incidence

The beaches of Rio de Janeiro city are generally highly exposed to strong swells from the southern quadrants (67.2% of the coastline) due to the predominantly east-west orientation of the coastline. However, wave direction and the presence of islands and rocky shores cause some beaches to be more or less exposed under specific conditions (Figs. 1 and 2). This variability is captured by indicator a.

Three segments deviate from the general classification: RBT-3, RBT-8, and the entire Copacabana–Leme beach arc, which collectively represent 31.4% of the study area. In RBT-3, beachrocks in the foreshore provide additional protection, reducing wave exposure. In RBT-8, the Tijucas Islands serve as a natural barrier. The Copacabana–Leme arc, with its SW-NE orientation, offers greater protection from high-energy swells originating from the SW.

b) Wave Collision Potential

Overall, the study area exhibits a moderate potential (51.8%) for wave collision, followed by low (22.7%), very low (20.0%), and high (4.1%) potential levels. Notable sectors with very low potential include RBT-1, RBT-5, and RBT-7. In opposition, the only sector classified with high potential is LIA-1.

These outcomes are primarily influenced by variations in foreshore slope, which affect wave run-up and its interaction with beach width, dune base elevation (when present), and backshore features.

c) Foreshore slope

Steeper foreshore slopes are associated with higher wave run-up on the beach profile (Sallenger 2000). In this study, steeper slopes were assigned a higher contribution to the overall vulnerability score.

Across the study area, foreshore slopes range from moderate (7% to 10.5%, representing 17.7% of the area), to high (10.5% to 14%, 44.2%), and very high (above 14%, 36.6%). The gentlest slopes are found in sectors CLA-1, RBT-7, and CLA-2, while the steepest slopes occur in MCB-1, RBT-3, and RBT-2.

• Synthesis of Ex Results

The synthesis of all indicators (Figs. 3 and 4) reveals that the study area predominantly exhibits a moderate degree of exposure (35.2%) to storm impacts, followed by high (32.7%), very high (27.5%), and low (3.2%) exposure levels. Notably, no segments were classified with a very low degree of exposure.

The highest exposure levels were recorded in segments MCB-1, RBT-2, RBT-4, LIA-1, and LIA-4. In contrast, RBT-7 was identified as the segment with the lowest exposure, primarily due to its very low wave collision potential, semi-exposed orientation, and moderate foreshore slope.

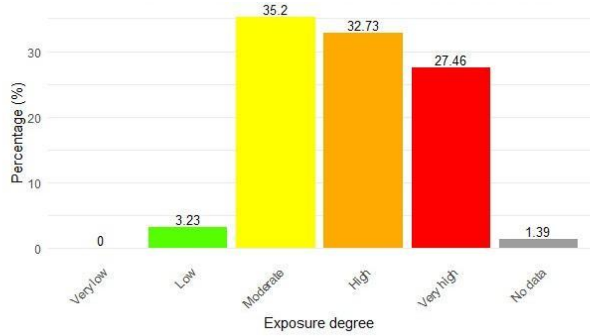


Figure 3: Percentage of each exposure degree along the coastline of Rio de Janeiro city between Leme and Macumba beaches.

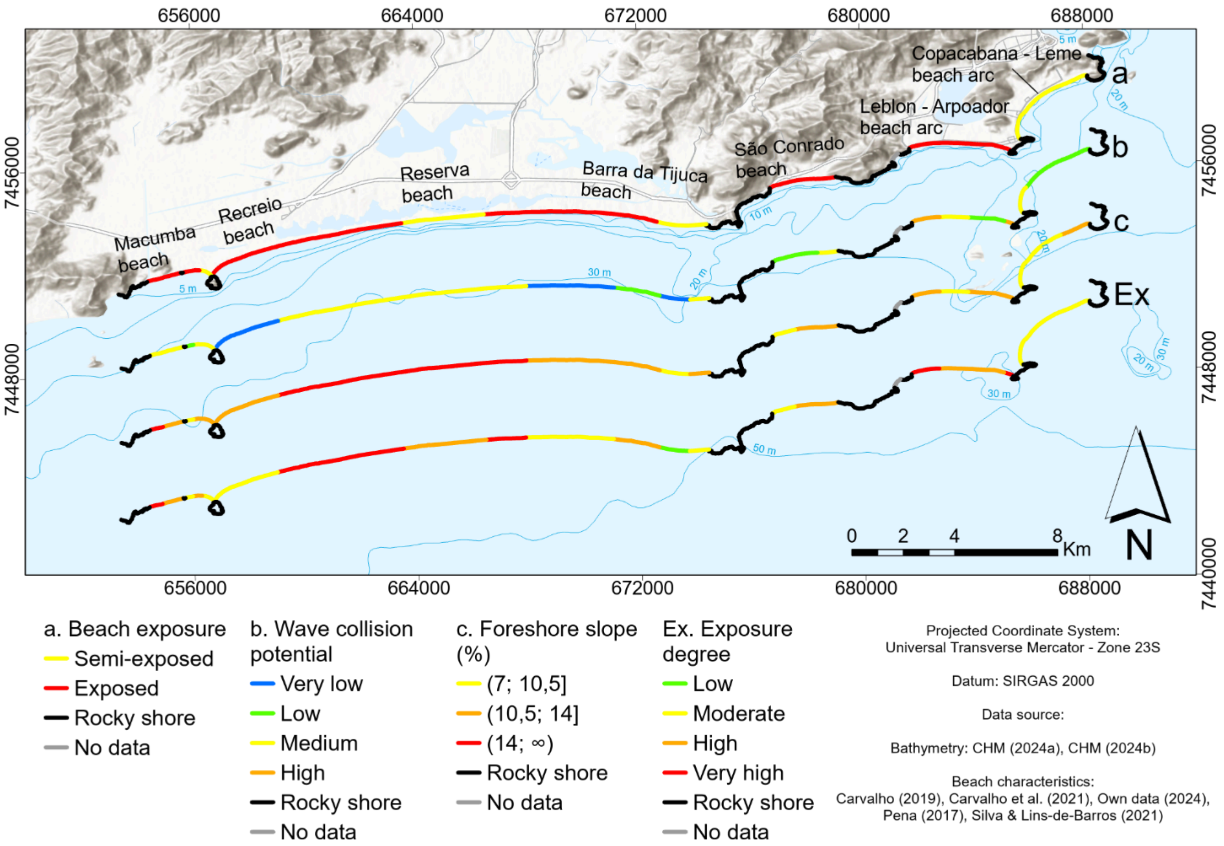


Figure 4: Characteristics of Rio de Janeiro’s coastline according to the Exposure subindex (Ex) variables.

### 4.2 AC subindex

d) Grain size

The study area predominantly features medium-sized sand grains (91.6%). The exception is Macumba Beach, which contains coarse sand grains (7.0%), providing this beach arc with greater resistance to storm surges based on this indicator.

e) Back beach elevation

Back beach elevation varies across the study area, ranging from high altitudes above 6 m (21.7%) to low altitudes below 3 m (6.2%). The most common elevations are between 5 and 6 m (45.7%). This indicator directly correlates with storm damage, such as erosion and wave overtopping (Sallenger 2000). Areas like LIA-2 and CLA-1, where such events are frequent, have lower back beach elevations.

f) Back beach feature

In the back beach zones of the study area, frontal dunes — either vegetated (49.8%) or degraded (19.2%) — and urbanized areas (29.5%) are predominant. Beaches in South Zone (São Conrado, Leblon-Ipanema-Arpoador, and Copacabana–Leme arcs) exhibit the highest levels of anthropization, correlating with increased reports of storm surge damages (Lins-de-Barros et al. 2018). Similarly, urbanized segments of Macumba Beach have also faced repeated storm-induced infrastructure damage (Pereira et al. 2018).

g) Protective Width slope

The study area predominantly exhibits protective width slopes exceeding 4% (85.5% of the area). The gentlest slopes are found in the Copacabana–Leme arc (CLA-2 and CLA-3). These low slopes are associated with recurrent wave overtopping and flooding during storm events (Silva & Lins-de-Barros 2021).

h) Beach width

Beach widths in the study area generally range between 25 and 100 m (93.8%). Narrow sections are found in Macumba Beach, RBT-5, SCB-3, and CLA-1. Medium and wide segments are most prevalent in Recreio and Reserva. Wider beaches are observed in sectors RBT-1, RBT-8, LIA-2, LIA-3, and CLA-3, with CLA-2 having the widest stretches. The greatest widths in Copacabana-Leme arc is due to artificial sand nourishment projects completed in the late 1960s, which have maintained high sediment volumes to this day (Silva & Lins-de-Barros 2021).

- Synthesis of AC Results

Overall, the study area demonstrates high adaptive capacity to storm surge impacts according to the selected indicators. Macumba Beach alternates between high and moderate capacity due to its combination of coarse sediment, moderate back beach elevation, and vegetated frontal dunes interspersed with urbanized backshore areas. However, its central section exhibited low resistance, a historically vulnerable area repeatedly affected by storm surges (Pereira et al. 2018).

The final results for this subindex (Figs. 5 and 7) show that the Recreio-Reserva–Barra da Tijuca arc mostly displays high adaptive capacity to storm events, except for sector RBT-8, which is rated moderate. In RBT-8, the lower slope of the protective width contributes to reduced adaptive capacity.

By contrast, the South Zone's beaches exhibited the lowest adaptive capacities. São Conrado Beach showed variation, with low capacity in SCB-3 and high capacity in SCB-2. The Leblon-Ipanema-Arpoador arc displayed a range from high capacity in LIA-3 to low capacity in LIA-2. Copacabana–Leme consistently demonstrated low adaptive capacity throughout its extent, influenced by low back beach elevation, gentle slopes, and significant anthropization.

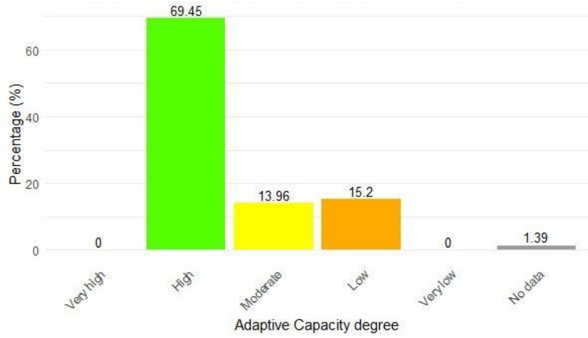


Figure 5: Percentage of each adaptive capacity degree along the coastline of Rio de Janeiro city between Leme and Macumba beaches.

### 4.3. Beach Vulnerability Index (BVI)

The final result of the Beach Vulnerability Index (Figs. 6 and 9) indicates that 3.2% of the coastline exhibits low vulnerability, 17.6% shows low to moderate vulnerability, 31.5% moderate vulnerability, 38.3% moderate to high vulnerability, and 7.9% high vulnerability. The sections with high vulnerability are located at Macumba, Leblon, and Arpoador beaches.

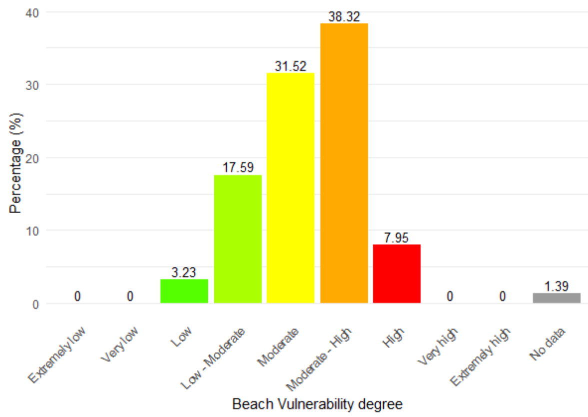


Figure 6: Percentage of each beach vulnerability degree along the coastline of Rio de Janeiro city between Leme and Macumba beaches.

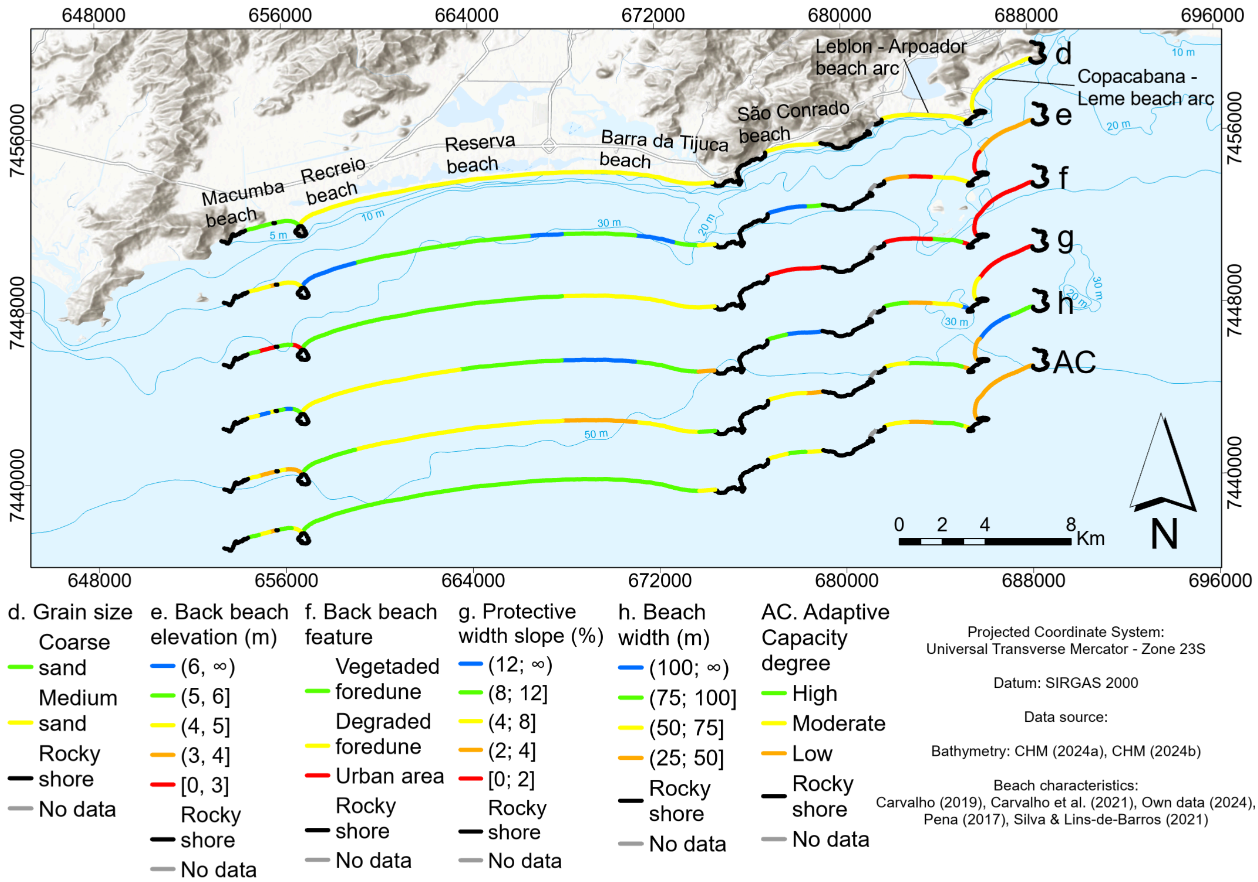


Figure 7: Characteristics of Rio de Janeiro's coastline according to the Adaptive Capacity subindex (AC) variables.

## 5. Discussion

### 5.1 BVI and Previous Observations

The results of this study align closely with patterns observed in previous research and field data, including topographic monitoring of the beaches conducted between 2016 and 2024. A historical inventory of storm surge reports published in O Globo newspaper between 1948 and 2008 (Lima 2022, Lins-de-Barros et al. 2018) identified Leblon Beach as the most frequently affected, with over 100 storm surge events documented during the study period.

As illustrated in Figure 8, 44.8% of reported negative impacts from storm surges occurred in segments classified as highly vulnerable, while 35.7% were recorded in areas categorized as having moderate to high vulnerability. The remaining 19.5% of impacts were associated with segments exhibiting moderate vulnerability. The most frequently reported effects included sand deposition on roadways, overwash events, flooding in urbanized areas, and, less frequently, structural damage to kiosks, sidewalks, and bike paths (Fig. 10).

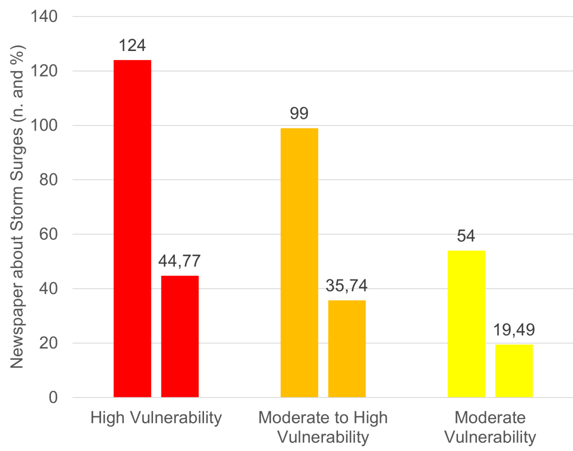


Figure 8: Negative impacts of storm surges reported by O Globo newspaper (1948–2008) in segments of the study area, classified by degree of vulnerability. The number of reported instances of negative impacts was sourced from Lima (2022).

Pena (2017) identified a general trend of stability across the Leblon–Ipanema–Arpoador beach arc but noted the occurrence of erosional pulses at its western and eastern extremities, corresponding to the LIA-1 and LIA-4 sectors, respectively. These data align with the present study's findings, which classified these sectors as having the highest vulnerability within the study area. At São Conrado Beach, Pena (op. cit.) observed stable conditions in sectors SCB-1 and SCB-2, whereas sector SCB-3 exhibited a clear erosive trend. This observation is consistent with the present study's classification of SCB-3 as having moderate to high vulnerability.

At Macumba Beach, the sectors MCB-1 to MCB-3, classified as having Moderate to High and High vulnerability, are the same areas where more severe erosive episodes with infrastructure damage were identified by Pereira et al. (2018). Pena (2017) also identified an erosive trend for the section corresponding to MCB-3. However, the author identified a trend of stability for the rest of the beach, which corresponds to the result found in the index for these sections.

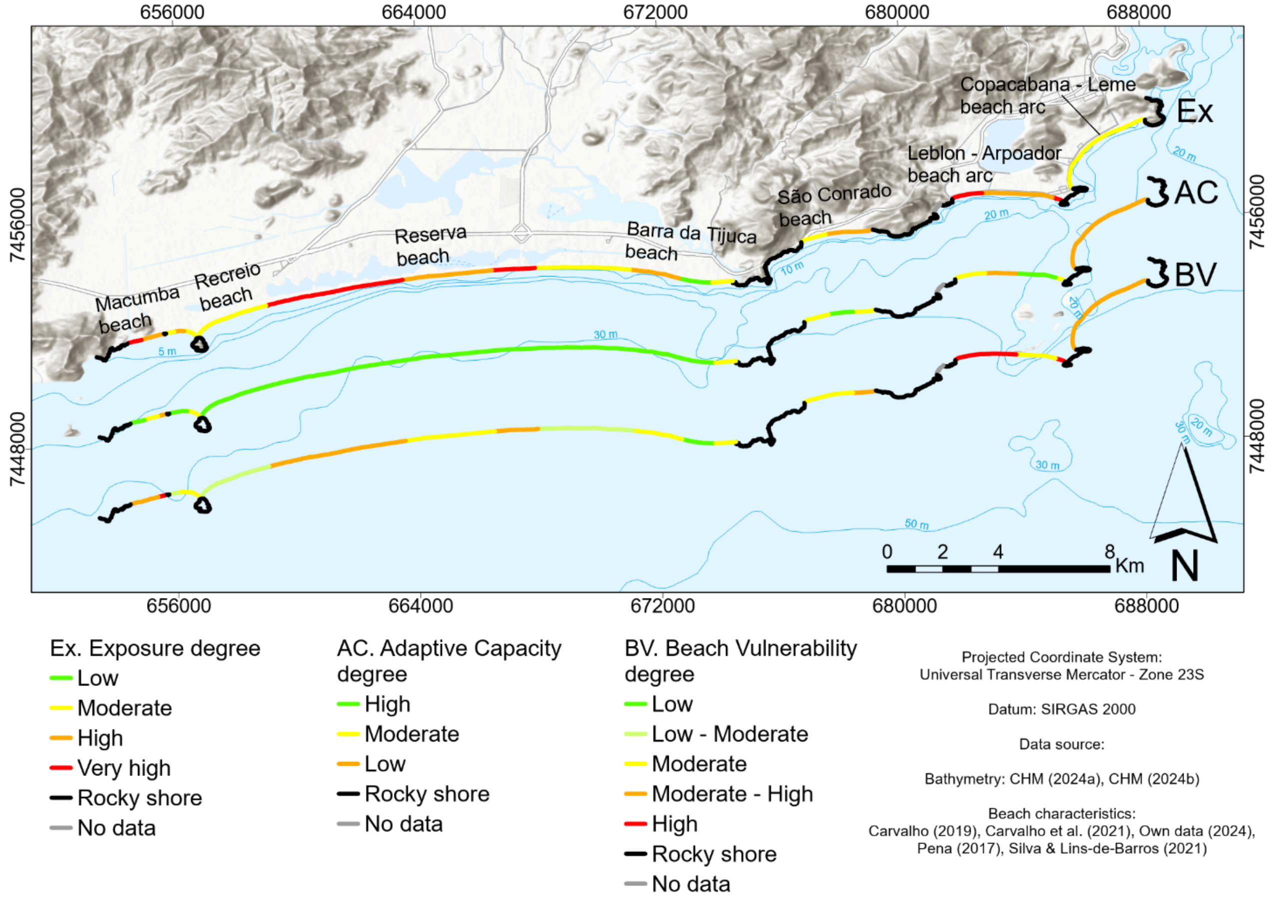


Figure 9: Rio de Janeiro's coastline according to the Beach Vulnerability Index (BVI)

### 5.2 Urban Occupation and Social Data

Anthropogenic alterations in the coastal occupation of densely urbanized areas have significantly transformed natural barriers, including the destruction of frontal dunes and coastal vegetation. These changes have lowered the elevation of the backshore and altered beach slopes (Lins-de-Barros et al. 2019). The replacement of dunes and coastal vegetation with man-made structures, such as walls and staircases, has weakened natural barriers, reducing the resilience of beaches to sea-level rise because the reduction of natural function exerted by the dunes (Johnston et al. 2023, Van de Biest et al. 2017) — a phenomenon observed not only in Rio de Janeiro (Lins-de-Barros et al. op. cit.) but also in other coastal cities in Brazil and globally. Given that urbanized areas and degraded dunes represent a reduction in the beach's physical capacity for resistance and adaptation, their presence was included in the formulation of the AC subindex as types of backshore features.

The proposed index does not incorporate other anthropogenic data, such as population density or income levels, despite their inclusion in prior studies on coastal vulnerability indices (Pires et al. 2012, Wamsley et al. 2015, De Serio et al. 2018, McLaughlin & Cooper 2010), including previous research conducted in the state of Rio de Janeiro (Lins-de-Barros 2010, Lins-de-Barros 2017, Lins-de-Barros & Muehe 2013). In Rio de Janeiro city, for instance, Carvalho & Guerra (2023) incorporated both geomorphological and oceanographic variables alongside population density to assess vulnerability in the coastal stretch between Marambaia and Barra da Tijuca. Their findings revealed high vulnerability in the eastern segment of Barra da Tijuca, corresponding to the most densely occupied area.

While the relevance of social factors is acknowledged — given their utility in estimating social impacts and financial losses from extreme events — this analysis focuses on identifying areas with the greatest physical susceptibility to negative impacts from storm surges. Including variables such as population density or average income could obscure physical vulnerability patterns. For example, the high-income area of Leblon Beach might appear less vulnerable despite its susceptibility to erosion and storm surge impacts. On the other hand, beaches such as Recreio, and sections of Macumba, Reserva and Barra da Tijuca, which are classified as having low to moderate physical vulnerability, might appear more exposed when population density is factored in, as presented by Carvalho & Guerra (2023). However, considering only the physical conditions, this section does not have a strong potential for width reduction or greater impacts from storm surges.


Figure 10: Examples of damages observed at the study area's beaches. a) Destruction of the promenade at Macumba Beach in October 2017 (O Globo 2017); b) Erosional episode at Post 8, Barra da Tijuca Beach, in August 2020 (G1 Rio 2020); c) Beach access ramp destroyed at São Conrado Beach in 2016 (G1 Rio 2016); d) Cleanup crews and reporters covering overwash events at Post 11, Leblon Beach, in August 2024. Source: Personal collection; e) Narrow beach width following a storm surge event at Copacabana Beach in July 2018 (Extra 2018).

In contrast, population exposure indicates the segments of the coastline with the highest number of people at risk from the effects of storm surges. Census data from IBGE (2022a) linked to coastal vulnerability classifications reveal that 22,124 people (46.6% of the total coastal population in the study area) reside in areas with high or moderate-to-high vulnerability. A total of 12,597 people (26.6%) inhabit areas classified as moderate vulnerability, while 12,722 people (26.8%) reside in areas with moderate-to-low or low vulnerability (Fig. 11).

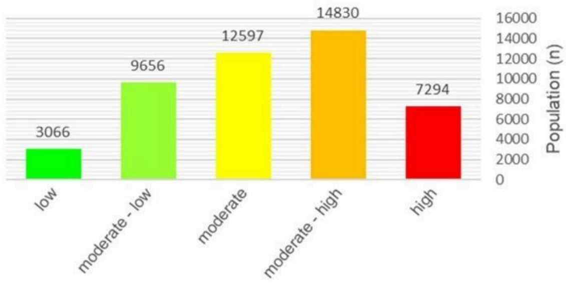


Figure 11: Total resident population (2022) on the seashore in the segments classified according to vulnerability between Leme and Macumba beaches (RJ). Source: IBGE (2022a).

### 5.3 Sediment Stock Recovery and Resilience

Although the resilience component is not addressed in the index, it is important to note that despite the severe impacts caused by storm surge events in some coastal areas, many beaches demonstrate a strong capacity to recover their sediment stock. These beaches do not exhibit evidence of shoreline retreat, indicating an absence of continuous coastal erosion. This recovery capacity was observed in monitoring conducted by the Marine Geography Laboratory of UFRJ in the RBT and LIA beach arcs.

For instance, following a severe storm surge in August 2024, the first beach arc experienced a sediment stock reduction exceeding 20%. The second arc, in turn, showed retreat rates of up to 80%. On average, the beaches returned to their typical volume conditions within a period of 2 to 7 weeks.

## 6. Conclusions

The Beach Vulnerability Index (BVI) presented in this study provides critical insights for identifying the main hotspots of potential impacts from storm surge events, offering valuable support for the management of Rio de Janeiro's beaches. Considering the complex morphodynamics, exposure to oceanographic and meteorological events, and the immense social value of beaches, the results herein contribute to addressing the challenge of forecasting storm surges with the potential for negative impacts.

One potential application of this index is its use in identifying key indicators for the development of an early-warning system for storm surge impacts, as well as informing decisions regarding interventions related to coastal erosion. A clear understanding of the geomorphological attributes that amplify or diminish beach vulnerability is essential for projecting potential scenarios during future extreme events. It is worth emphasizing that the vulnerability conditions presented in this study indicate the potential for adverse effects should storm surges occur. However, variations in wave conditions — such as height, direction, period, and astronomical or meteorological tides — can significantly influence the intensity and spatial distribution of impacts across individual beaches.

Thus, to develop and to enhance the predictive accuracy of a storm surge impact warning system, this analysis should be complemented with real-time monitoring of beach conditions immediately prior to such events. While the index is based on average geomorphological parameters, offering a baseline understanding of the typical behavior of each beach, the dynamic nature of coastal geomorphology necessitates real-time assessments of parameters such as beach slope, width, and backshore elevation. The importance of this analysis lies in allowing a dual approach, comparing average conditions with real-time data, which has the potential to refine impact predictions and enable the prioritization of vulnerable areas requiring immediate attention during extreme events.

Regarding coastal erosion, the study emphasizes that beaches exhibiting higher vulnerability to storm surges may serve as priority areas for monitoring and intervention, particularly under scenarios of climate change. Understanding the drivers of increased or decreased vulnerability is essential for projecting future scenarios, not only in the context of rising sea levels and more frequent extreme events but also considering anthropogenic alterations to natural coastal barriers, backshore elevations, and other critical physical parameters. The results further highlight that many beaches demonstrate substantial adaptive capacity, suggesting opportunities for urban occupation adjustments that reduce the need for engineered solutions. Instead, priority could be given to nature-based interventions, such as establishing protective zones, restoring natural barriers, and implementing ecosystem-based strategies.

The findings also reveal that the degradation or removal of frontal dunes and coastal vegetation has significantly heightened vulnerability in certain areas by diminishing the natural resistance to storm surge impacts. Immediate measures to restore and maintain these ecosystems are critical, particularly in areas with lower vulnerability, where the preservation of these features can play a preventative role. Furthermore, in regions with relatively intact dunes and vegetation, careful urban planning is imperative to prevent the degradation of these essential coastal ecosystems, ensuring their continued function as natural protective barriers.

Finally, this study stresses the urgent need to incorporate coastal vulnerability assessments into formal coastal management frameworks, such as the Orla Project and the Municipal Coastal Management Plan, both of which have yet to be implemented in Rio de Janeiro. Integration into the city’s master plan is also critical for fostering sustainable coastal management and ensuring the long-term adaptive capacity of these valuable coastal zones.

## Acknowledgments

The authors are grateful to CAPES for the master's scholarship, to FAPERJ for supporting the research (grant number E-26/211.555/2021), to UFRJ for the undergraduate research scholarships, and to CNPq for the Research Productivity Fellowship (grant number 307292/2023-1). We also thank the reviewers for their comments, Professors Josefa Varela Guerra and Mauro Cirano for their contributions to the development of this work, and the members of the Marine Geography Laboratory at UFRJ who took part in the fieldworks, especially Hugo Diniz Brandão.

## Credit author statement

P.A.S.P.: Conceptualization, Methodology, Investigation, Data curation, Formal analysis, Writing - original draft preparation, Writing - review and editing.

F.M.L.-B.: Conceptualization, Methodology, Investigation, Data curation, Formal analysis, Writing - original draft preparation, Writing—review and editing, Supervision, Validation, Project administration, Resources, Funding acquisition.

P.T.C.: Investigation, Writing—original draft preparation, Writing—review and editing.

## References

ADGER W.N.; BROOKS N.; BENTHAM G.; AGNEW M.; ERIKSEN S. 2004. New indicators of vulnerability and adaptive capacity. Available at: https://www.researchgate.net/publication/257343107_New_Indicators_of_Vulnerability_and_Adaptive_Capacity. Accessed on November 11, 2024.

ALEXANDRAKIS G.; POULOS S.E. 2014. An holistic approach to beach erosion vulnerability assessment. Scientific Reports, 4: 1-8. 10.1038/srep06078.

ANDRADE T.S.; SOUSA P.H.G.O; SIEGLE E. 2019. Vulnerability to beach erosion based on a coastal processes approach. Applied Geography, 102:12-19. https://doi.org/10.1016/j.apgeog.2018.11.003.

ANAZAWA T M, FEITOSA F F, MONTEIRO A M V, ALFAYA F A V. S. 2011. Análise preliminar das áreas em situação de vulnerabilidade socioambiental de São Sebastião (Litoral Norte, SP). Anais XV Simpósio Brasileiro de Sensoriamento Remoto – SBSR, 1012–1019. Available at:

http://marte.sid.inpe.br/col/dpi.inpe.br/marte/2011/06.29.17.18/doc/p0378.pdf. Accessed on July 15, 2025

BIRD E. 2008. Coastal Geomorphology: An Introduction. John Wiley & Sons, Ltd, 411p.

BULHÕES E. 2006. Condições Morfodinâmicas Associadas a Riscos aos Banhistas. Contribuição à Segurança nas Praias Oceânicas da Cidade do Rio de Janeiro, RJ. Master's thesis. Graduate studies in Geography, Department of Geography, Federal University of Rio de Janeiro (UFRJ).

CALEFFI F.; VIEGAS C.V.; LIMA K.B.; BONATO S.V. 2024. Os impactos de eventos climáticos extremos: uma análise abrangente das enchentes de 2024 no Rio Grande do Sul. Redes, 29(1):1–27. https://doi.org/10.17058/redes.v29i1.19660.

CARVALHO B.C. 2019. Variabilidade da resposta da linha de costa aos condicionantes hidrodinâmicos e às oscilações do nível do mar no litoral sul fluminense. PhD thesis. Graduate studies in Oceanography, Faculty of Oceanography, Rio de Janeiro State University (UERJ), 192p.

CARVALHO B.C.; GUERRA J.V. 2020. Coastal vulnerability of Rio de Janeiro shoreline (SE Brazil) due to natural and social impacts. Journal of Coastal Research, 95:759-763. https://doi.org/10.2112/SI95-148.1.

CARVALHO B.C.; GUERRA J.V. 2023. Estudo das mudanças na linha de costa e vulnerabilidade costeira associada no litoral sul do Rio de Janeiro (SE Brasil). Revista Cartográfica, 107:11-34. https://doi.org/10.35424/rcarto.i1070.2421

CARVALHO B.C.; LINS-DE-BARROS F.M.; SILVA P.L.; PENA J.N.; GUERRA J.V. 2021. Morphological variability of sandy beaches due to variable oceanographic conditions: a study case of oceanic beaches of Rio de Janeiro city (Brazil). Journal of Coastal Conservation, 25:1-16. 10.1007/s11852-021-00821-8.

CHM. 2024a. Carta Náutica Raster nº 1506 – Proximidades da Baía de Guanabara. Centro de Hidrografia da Marinha. Available at: https://www.marinha.mil.br/chm/dados-do-segnav/cartas-raster. Accessed on July 10, 2025.

CHM. 2024b. Carta Náutica Raster nº 1620 – Do Pontal de Sernambetiba à Ilha Grande. Centro de Hidrografia da Marinha. Available at: https://www.marinha.mil.br/chm/dados-do-segnav/cartas-raster. Accessed on July 10, 2025.

CUTTER, S.L. 2011. A ciência da vulnerabilidade: modelos, métodos e indicadores. Revista Crítica de Ciências Sociais, 93:59–69. https://doi.org/10.4000/rccs.165.

DE SERIO F.; ARMENIO E.; MOSSA M.; PETRILLO A.F. 2018. How to define priorities in coastal vulnerability assessment. Geosciences, 8:1-20. https://doi.org/10.3390/geosciences8110415.

DIAS G.T.M.; KJERFVE B. 2009. Barrier and Beach Ridge Systems of the Rio de Janeiro Coast. In: DILLENGURG S.R., HESP P. (eds) Lecture Notes in Earth Sciences; Springer, Berlin, Heidelberg, 225-252p. https://doi.org/10.1007/978-3-540-44771-9_7.

DIAS T. 2024. Enchentes no RS: leia o relatório de 2015 que projetou o desastre – e os governos decidiram engavetar. Intercept Brasil. Available at: https://www.intercept.com.br/2024/05/06/enchentes-no-rs-leia-o-relatorio-de-2015-que-projetou-o-desastre-e-os-governos-escolheram-engavetar. Accessed on July 16, 2025.

DOLAN R.; DAVIS R.E. 1992. An intensity scale for Atlantic coast northeast storms. Journal of Coastal Research, 8:840-853.

DONG Z.; ELKO N.; ROBERTSON Q.; ROSATI J. 2018. Quantifying beach and dune resilience using the coastal resilience index. Coastal Engineering Proceedings, 1:1-8. https://doi.org/10.9753/icce.v36.papers.30.

EXTRA. 2018. Ressaca faz sumir quase toda faixa de areia no Posto 6, em Copacabana. Available at: https://extra.globo.com/rio/ressaca-faz-sumir-quase-toda-faixa-de-areia-no-posto-6-em-copacabana-23139416.html. Accessed on December 11, 2022.

FERNANDEZ, G.B.; MALUF, V.; BULHÕES, E.M.; ROCHA, T.B.; PEREIRA, T.G.; FILHO, S.O. 2015. Impactos morfológicos e resiliência das praias do litoral do Rio de Janeiro: referência especial à morfodinâmica praial. In: PAULA, D.P.; DIAS, J.A. (orgs) Ressacas do mar/temporais e gestão costeira. Premius, Fortaleza, 277-329p. ISBN: 978-85-7924-440-7.

FILHO S.R.O.; SANTOS R.A.; FERNANDE G.B. 2020. Erosão e recuperação de praias refletivas de alta energia impactadas por ondas de tempestade geradas por ciclone tropical. Revista Brasileira de Geomorfologia, 21:289-312. https://doi.org/10.20502/rbg.v21i2.1455.

G1 RIO. 2016. Após reforma, Rio Águas disse que calçadão era 'à prova de ressaca'. Available at: https://g1.globo.com/rio-de-janeiro/noticia/2016/05/apos-reforma-rio-aguas-disse-que-calcadao-era-prova-de-ressaca.html. Accessed on December 20, 2022.

G1 RIO. 2020. Ressaca destrói parte do calçadão na Barra da Tijuca, Zona Oeste do Rio. Available at: https://g1.globo.com/rj/rio-de-janeiro/noticia/2020/08/22/ressaca-destroi-parte-do-calcadao-na-barra-da-tijuca-zona-oeste-do-rio.ghtml. Accessed on June 20, 2024.

G1 RS. 2025. Mais de 180 mortos, 25 desaparecidos e 96% das cidades atingidas: o raio-X da enchente que devastou o RS um ano após tragédia. G1. Available at: https://g1.globo.com/rs/rio-grande-do-sul/1-ano-de-enchente-rs/noticia/2025/04/29/mais-de-180-mortos-25-desaparecidos-e-96percent-das-cidades-atingidas-o-raio-x-da-enchente-que-devastou-o-rs-um-ano-apos-tragedia.ghtml. Accessed on July 16, 2025.

G1 VALE DO PARAÍBA E REGIÃO. 2023. Temporal devastador no Litoral Norte de SP completa um mês; confira um resumo da tragédia. G1. Available at: https://g1.globo.com/sp/vale-do-paraiba-regiao/noticia/2023/03/19/temporal-devastador-no-litoral-norte-de-sp-completa-um-mes-confira-um-resumo-da-tragedia.ghtml. Accessed on July 15, 2025.

GORNITZ V. 1991. Global coastal hazards from future sea level rise. Palaeogeography, Palaeoclimatology, Palaeoecology, 89:379-398. https://doi.org/10.1016/0031-0182(91)90173-O.

HARLEY M. 2017. Coastal Storm Definition. In: CIAVOLA P.,; COCO G. (eds) Coastal Storms: Processes and Impacts. Wiley Blackwell, 1–21.

HINKEL J.; KLEIN R.J.T. 2009. Integrating knowledge to assess coastal vulnerability to sea-level rise: The development of the DIVA tool. Global Environmental Change, 19:384-395. https://doi.org/10.1016/j.gloenvcha.2009.03.002.

IBGE. 2022a. Censo 2022. Instituto Brasileiro de Geografia e Estatística. Available at: https://www.ibge.gov.br/estatisticas/sociais/trabalho/22827-censo-demografico-2022.html. Accessed on November 11, 2024.

IBGE. 2022b. Malha das Unidades Federativas do Brasil. Rio de Janeiro: Instituto Brasileiro de Geografia e Estatística. Available at: https://www.ibge.gov.br/geociencias/downloads-geociencias.html. Accessed on January 10, 2024.

IBGE. 2022c. Malha municipal do Rio de Janeiro. Rio de Janeiro: Instituto Brasileiro de Geografia e Estatística. Available at: https://www.ibge.gov.br/geociencias/downloads-geociencias.html. Accessed on January 10, 2024.

IPCC. 2023. Climate Change 2023: Synthesis Report. IPCC, Geneva, Switzerland, 1–184. https://doi.org/10.59327/IPCC/AR6-9789291691647.

JOHNSTON K.; DUGAN J.E.; HUBBARD D.M.; KYLE A. 2023. Using dune restoration on an urban beach as a coastal resilience approach. Frontiers in Marine Science, 10:1-17. https://doi.org/10.3389/fmars.2023.1187488.

KLUMB-OLIVEIRA L. 2024. The climatology and classification of coastal storms on the Southeastern coast of Rio de Janeiro State, Brazil. Ocean and Coastal Research, 72:1-17. https://doi.org/10.1590/2675-2824072.23081.

KOMAR P.D.; MILLER M.C. 1973. The threshold of sediment movement under oscillatory water waves. Journal of Sedimentary Petrology. 1973, 43:1101-1110.

LIMA R.F. 2022. Caracterização das ressacas do mar e seus efeitos no litoral do estado do Rio de Janeiro. Master's thesis. Graduate studies in Geography, Department of Geography, Federal University of Rio de Janeiro (UFRJ).

LIMA R.F., LINS-DE-BARROS F.M.; CIRANO M. 2021. Análise das Condições Meteoceanográficas em Eventos de Ressaca do Mar no Litoral do Estado do Rio de Janeiro, Brasil no Período de 1948 e 2008, Anuário do Instituto de Geociências, 44:1-12. https://doi.org/10.11137/1982-3908_2021_44_41726.

LINS-DE-BARROS F.M. 2010. Contribuição metodológica para análise local da vulnerabilidade costeira e riscos associados: estudo de caso da Região dos Lagos, Rio de Janeiro. PhD thesis. Graduate studies in Geography, Department of Geography, Federal University of Rio de Janeiro (UFRJ), 297p.

LINS-DE-BARROS, F.M. 2017. Integrated coastal vulnerability assessment: A methodology for coastal cities management integrating socioeconomic, physical and environmental dimensions - Case study of Região dos Lagos, Rio de Janeiro, Brazil. Ocean & Coastal Management, 149:1-11. https://doi.org/10.1016/j.ocecoaman.2017.09.007.

LINS-DE-BARROS, F.M., MUEHE D. 2013. The Smartline Approach to Coastal Vulnerability and Social Risk Assessment Applied to a Segment of the East Coast of Rio de Janeiro State, Brazil. Journal of Coastal Conservation, 17:211-223. https://doi.org/10.1007/s11852-011-0175-y.

LINS-DE-BARROS, F.M.; KLUMB-OLIVEIRA L.; LIMA R. F. 2018. Avaliação histórica da ocorrência de ressacas marinhas e danos associados entre os anos de 1979 e 2013 no litoral do estado do Rio de Janeiro (Brasil). Revista de Gestão Costeira Integrada/Journal of Integrated Coastal Zone Management, 18:85-102. https://doi.org/10.5894/rgci-n146.

LINS-DE-BARROS, F.M.; PARENTE-RIBEIRO L. 2018. How Much Is a Beach Worth: Economic Use and Vulnerability to Coastal Erosion: The Case of Ipanema and Arpoador Beaches, Rio de Janeiro (Brazil). In: FILHO W.L.; FREITAS L.E. (eds) Climate Change Adaptation in Latin America: Managing Vulnerability, Fostering Resilience. Springer, Cham, 207-222p.

LINS-DE-BARROS, F.M., PAULA D.P.; SOUSA P.H.G.O. 2020. Vulnerabilidade costeira: conceitos, abordagens e aplicações. In: MUEHE D., LINS-DE-BARROS F.M., PINHEIRO L. (eds) Geografia Marinha: oceanos e costas na perspectiva de geógrafos. PGGM, Rio de Janeiro, 631-654p.

LINS-DE-BARROS F.M., SAUZEAU T.; GUERRA J.V. 2019. Historical evolution of seafront occupation in France (Bay of Biscay) and Brazil (Rio de Janeiro) face to coastal erosion vulnerability and risks (19th - 21th centuries). Confins, 39:1-36. https://doi.org/10.4000/confins.18175.

MARANDOLA JR. E.; MARQUES C.; PAULA L.T.; CASSANELI L.B. 2013. Crescimento urbano e áreas de risco no litoral norte de São Paulo. Revista Brasileira de Estudos de População, 30(1):35–56. https://doi.org/10.1590/S0102-30982013000100003.

MARENGO J.A.; DOLIF G.; CUARTAS A.; CAMARINHA P.; GONÇCALVES D.; LUIZ R.; SILVA L.; ALVALA R.C.S.; SELUCHI M.E.; MORAES O.L.; SOARES W.R.; NOBRE C.A. 2024. O maior desastre climático do Brasil: chuvas e inundações no estado do Rio Grande do Sul em abril-maio 2024. Estudos Avançados, 38(112):203–228. https://doi.org/10.1590/s0103-4014.202438112.012.

MARTH J.D.; MOURA N.S.V.; KOESTER E. 2016. Estudo da suscetibilidade à inundação com base em análise geomorfológica, bacia hidrográfica do Arroio Santa Isabel, região costeira do Rio Grande do Sul, Brasil. Revista do Instituto Geológico, 37(1):13–28. https://doi.org/10.5935/0100-929X.20160002.

MARTIN L.; BITTENCOURT A.C.S.P.; VILAS-BOAS G.S. 1982. Primeira ocorrência de corais pleistocênicos da costa brasileira - datação do máximo da penúltima transgressão. Ciências da Terra, 3:16–17.

MCFADDEN L. 2007. Vulnerability analysis: a useful concept for coastal management? In: MCFADDEN L., NICHOLLS R., PENNING-ROWSELL E. (eds) Managing Coastal Vulnerability. Elsevier, Oxford, 15-28p.

MCLAUGHLIN S.; COOPER J.A.G. 2010. A multi-scale coastal vulnerability index: A tool for coastal managers? Environmental Hazards, 9:233-248. https://doi.org/10.3763/ehaz.2010.0052.

MOURA N.S.V.; MORAN E.F.; DIAS, T.S.; PARIS, G.; BORGES F.F. 2016. Expansão urbana sobre compartimentos de relevo suscetíveis à inundação: Zona Sul do município de Porto Alegre, Rio Grande do Sul. Pesquisas em Geociências, 43(3):299–310. https://doi.org/10.22456/1807-9806.78237.

MUEHE D. 2011. Erosão costeira - Tendência ou eventos extremos? O litoral entre Rio de Janeiro e Cabo Frio, Brasil. Journal of Integrated Coastal Zone Management, 11:315-325. 10.5894/rgci282.

MUEHE D.; LINS-DE-BARROS, F.M., BULHÕES E.M.R.; KLUMB-OLIVEIRA L.; PINTO N.; SPERLE M. 2018. Rio de Janeiro. In: MUEHE D. (eds) Panorama da Erosão Costeira no Brasil. MMA, Brasília, 478-545p.

MUEHE D.; VALENTINI E. 1998. O Litoral do Estado do Rio de Janeiro: uma caracterização físico-ambiental. FEMAR, Rio de Janeiro, 123p.

NASCIMENTO M.X. 2013. Análise das condições meteoceanográficas na região da Bacia de Santos. Master's thesis. Graduate studies in Ocean Engineering, COPPE, Federal University of Rio de Janeiro (UFRJ), 110p.

NEVES C.F.; MUEHE D.E.; VALENTINI E.M.; ROSMAN P.C.C. 2007. Estudo de Vulnerabilidades no Litoral do Estado do Rio de Janeiro Devido às Mudanças Climáticas: Relatório Final. Rio de Janeiro: Fundação COPPETEC.

O GLOBO. 2017. Ressaca na Praia da Macumba provoca novos estragos. Available at https://oglobo.globo.com/rio/ressaca-na-praia-da-macumba-provoca-novos-estragos-21984406. Accessed June 01, 2024.

OLIVEIRA R. 2025. Plano de reconstrução do RS avança devagar, sem transparência e não mira em prevenção. Agência Pública. Available at: https://apublica.org/2025/04/plano-de-reconstrucao-do-rs-avanca-devagar-sem-transparencia-e-nao-mira-em-prevencao/. Accessed on July 16, 2025.

PANTUSA D.; D'ALESSANDRO F.; RIEFOLO L.; PRINCIPATO F.; TOMASICCHIO G.R. 2018. Application of a Coastal Vulnerability Index: a case study along the Apulian coastline, Italy. Water, 10:1-16. https://doi.org/10.3390/w10091218.

PAULA D.P. 2012. Análise dos riscos de erosão costeira no litoral de Fortaleza em função da vulnerabilidade aos processos geogênicos e antropogênicos. PhD thesis. Marine, Earth and Environmental Sciences/Coastal Management specialization, University of Algarve (UALG), 335p.

PAULA D.P.; BENDÔ A.R.R.; LIMA I.F.P.; ALVES J.W.O. 2016. Mudanças de curto prazo no balanço sedimentar da Praia do Icaraí (Caucaia, Ceará) durante uma ressaca do mar. Scientia Plena, 12(4). https://doi.org/10.14808/sci.plena.2016.045301.

PAULA D.P.; FARRAPEIRA NETO C.A.; SOUZA M.A.L.; DIAS J.M.A. 2014. Alterações morfológicas na Praia do Icaraí (Caucaia-Ceará) após a construção de um dissipador de energia para controle da erosão costeira. Revista GEONORTE, 10(2):7–11.

PENA J.N. 2017. Dinâmica Geomorfológica das Praias Oceânicas Urbanas da Cidade do Rio de Janeiro e Impactos Associados a Ressacas do Mar: Uma Contribuição à Gestão Costeira. Master's thesis. Graduate studies in Geography, Department of Geography, Federal University of Rio de Janeiro (UFRJ), 130p.

PEÑA-ALONSO C.; FRAILE-JURADO P.; HERNÁNDEZ-CALVENTO L.; PÉREZ-CHACON E.; ARIZA E. 2017. Measuring geomorphological vulnerability on beaches using a set of indicators (GVI): A tool for management. Journal of Environmental Management, 204:230-245. https://doi.org/10.1016/j.jenvman.2017.08.053.

PEREIRA T.; SALIBA A.; LESSA A.C.; GUZZO A.; ASSIS S. 2018. Morfodinâmica praial e os episódios erosivos na praia da Macumba, cidade do Rio de Janeiro, RJ. Anais do XII SINAGEO. Available at: https://www.sinageo.org.br/2018/trabalhos/2/2-248-1646.html. Accessed on June 23, 2023.

PIRES I.; CRAVEIRO J.; ANTUNES O. 2012. Artificialização do solo e Vulnerabilidade Humana em duas zonas sujeitas a processos de erosão costeira: casos de estudo da Costa da Caparica e Espinho (Portugal). Journal of Integrated Coastal Zone Management, 12:277-290. 10.5894/rgci316.

RAMIERI E.; HARLEY A.; BARBANTI A.; SANTOS F.D.; GOMES A.; HILDEN M.; LAIHONEN P.; MARINOVA N.; SANTINI M. 2011. Methods for assessing coastal vulnerability to climate change. ETC CCA Technical Paper. Available at: https://www.eionet.europa.eu/etcs/etc-cca/products/etc-cca-reports/1/@@download/file/TP_1-2011.pdf. Accessed on December 11, 2021.

RODRIGUES M. 2024. Falta de manutenção e falhas de projeto impediram o sistema de contenção de cheias de proteger Porto Alegre. Pesquisa FAPESP. Available at: https://revistapesquisa.fapesp.br/falta-de-manutencao-e-falhas-de

-projeto-impediram-o-sistema-de-contencao-de-cheias-de-proteger-porto-alegre/. Accessed on July 16, 2025.
SALLENGER A.H. 2000. Storm Impact Scale for Barrier Islands. Journal of Coastal Research, 16:890-895.
SHARPLES C. 2006. Indicative Mapping of Tasmanian Coastal Vulnerability to Climate Change and Sea-Level Rise. Explanatory Report, 1:1-173.
SHARPLES C. MOUNT R. PEDERSEN T. LACEY M. NEWTON J. JASKIERNIAK D. WALLACE L. 2009. The Australian Coastal Smartline Geomorphic and Stability Map Version 1: project report. Manual and Data Dictionary. Available at: https://figshare.utas.edu.au/articles/report/The_Australian_Coastal_Smartline_Geomorphic_and_Stabililty_Map_Version_1_Project_Report/23165279. Accessed on September 15, 2021.
SILVA P.L. LINS-DE-BARROS F.M. 2021. A alimentação artificial da Praia de Copacabana (RJ) após 51 anos: Transformações geomorfológicas e dinâmica atual. Terra Brasilis, 16:1-26. https://doi.org/10.4000/terrabrasilis.9980.
SILVA P.L. LINS-DE-BARROS F.M. 2018. História Geomorfológica da Praia de Copacabana ao longo do século XX e análise preliminar da subida do nível do mar. Anais do XII SINAGEO. Available at: https://www.sinageo.org.br/2018/trabalhos/2/2-123-2073.html. Accessed on January 06, 2024.
UCHOA, L. 2024. A tragédia do Rio Grande do Sul já estava prevista, afirmam especialistas. Instituto de Estudos Avançados da Universidade de São Paulo (IEA-USP). Available at: https://www.iea.usp.br/noticias/a-era-da-emergencia-climatica. Accessed on July 16, 2025.
VAN DER BIEST K. DE NOCKER L. PROVOOST S. BOEREMA A. STAES J. MEIRE P. 2017. Dune dynamics safeguard ecosystem services. Ocean & Coastal Management, 149:148-158. https://doi.org/10.1016/j.ocecoaman.2017.10.005.
WAMSLEY TY V. COLLIER Z.A. BRODIE K. DUNKIN L.M. RAFF D. ROSATI J.D. 2015. Guidance for Developing Coastal Vulnerability Metrics. Journal of Coastal Research, 31:1521-1530. 10.2112/JCOASTRES-D-14-00015.1.
WOODWORTH P.L.; MELET A.; MARCOS M.; RAY R.D.; WÖPPELMANN G.; SASAKI Y.N.; CIRANO M.; HIBBERT A.; HUTHNANCE J.M.; MONSERRAT S.; MERRIFIELD M.A. 2019. Forcing factors affecting sea level changes at the coast. Surveys in Geophysics, 40:1351–1397. https://doi.org/10.1007/s10712-019-09531-1.
WRIGHT L.D. SHORT A.D. 1984. Morphodynamic Variability of Surf Zones and Beaches: A Synthesis. Marine Geology, 56:93-118. https://doi.org/10.1016/0025-3227(84)90008-2.
XAVIER G. 2023. Tragédia anunciada: os alertas do MP ignorados pelo poder público em São Sebastião. CartaCapital. Available at: https://www.cartacapital.com.br/sociedade/tragedia-anunciada-os-alertas-do-mp-ignorados-pelo-poder-publico-em-sao-sebastiao. Accessed on July 15, 2025.

[1]Recebido 23 de dezembro de 2024
Aceito 07 de agosto de 2025